Influence of the Weathering Degree on the Dispersion Susceptibility of Allophanic Soils

Ángela Marcela Castañeda Jaimes[1], *Julio Esteban* Colmenares Montañez[2], and *Livaniel* Viveros Rosero[3]

Universidad Nacional de Colombia, Department of Civil and Agricultural Engineering, Bogotá, D.C., Colombia
[1]acastanedaj@unal.edu.co

ABSTRACT

The behavior of allophanic soils is directly related to their fabric and structure. They are transformed according to their weathering degree through biogeochemical processes that may give rise to changes in the minerals. This paper investigated the influence of weathering degree on the susceptibility to dispersion in materials derived from volcanic ash soil in Armenia (Colombia). X-ray fluorescence (XRF) tests and scanning electron microscopy (SEM) tests were conducted to identify mineralogical composition and correlate it with the use of geochemical indices. Pinhole tests were developed on natural and compacted samples (with prior air and oven drying), to assess susceptibility to dispersion. It was found that the most weathered material exhibits lower susceptibility to internal erosion due to particle aggregation generated during the material alteration process. At similar dry density, natural materials present intermediate permeability values compared to compacted ones under both water content conditions. Samples dried in the air retain part of their structure and promote lower hydraulic conductivity values compared to samples dried in the oven, indicating that material alteration due to drying generates differences in porosity and hydraulic conductivity. The drying process at higher temperatures changes the material properties, eliminating the gel texture and hence the cementing bonds, inducing imminent changes in microporosity. The findings contribute to evaluating the application of allophanic soils for embankment construction, where the loss of cementation contributes to the degree of infiltration, reducing shear strength and affecting internal stability.

Keywords: allophanic soils; weathering degree; dispersion.

1. Introduction

Soil dispersion or internal erosion refers to the detachment and movement of particles caused by water flow. The tendency for soil dispersion depends mainly on the physicochemical variables of the soil: mineralogy, chemistry, and salts dissolved in pore water. Some factors can trigger erosive processes: the existence of a significant hydraulic gradient, differences in porosity-permeability in different soil horizons favoring horizontal circulation, and the presence of burrows, roots, or cracks (Nadal-Romero et al. 2011).

In residual natural soils, the degree of weathering can control susceptibility to dispersion, given the conditions of fabric and structure at different stages of alteration. In compacted soils, the loss of structure is typically significant, promoting greater susceptibility to internal erosion. This study evaluated the validity of this statement for allophanic soils. This aspect allows for the assessment of their application in slope construction, where the loss of cementation contributes to the degree of infiltration, shear strength, and internal stability.

Allophanic soils refer to materials derived from the weathering of volcanic ash whose behavior is predominantly governed by clay-allophane minerals (Wesley 2003). The formation of allophanic soils begins with volcanic ash as the parent material, which undergoes chemical alteration or weathering of minerals through various processes, predominantly leaching (Fiantis et al. 2010). These processes depend on external factors such as precipitation, topography, deposit thickness, temperature, and time (Smeck, Runge, and Mackintosh 1983).

The weathering sequence begins with the release of a large amount of silica from primary minerals. Part of this silica is leached from the soil immediately, and the remaining portion reacts to form secondary minerals as well as Al-humic complexes and iron oxides (Flórez and Parra 2009; Gasser, Juchler, and Sticher 1994).

Several authors suggest that the sequence of minerals generated in the weathering of soils derived from volcanic ash corresponds is the one depicted in Figure 1 (Wesley 2003).

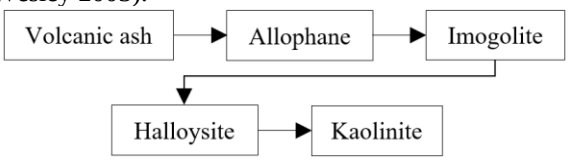

Figure 1. The mineral sequence in the weathering of allophanic soils (Adapted from Wesley 2003).

During the weathering of allophanic soils, supersaturated solutions that precipitate in the fine particle sizes favor the formation of poorly crystalline phases such as allophane and/or imogolite (Shoji, Nanzyo, and Dahlgren 1993). Allophane is composed of natural amorphous silicates and has physical characteristics very close to those of a synthetic gel (Parfitt 2009).

Allophanic soils are characterized by high organic matter contents, which are hosted in the amorphous

minerals and can be associated with low permeabilities. According to some studies, it has been found that at the scale of allophanic aggregates, the calculated permeability is low, which could be explained by a high organic matter content. Due to this condition, fluid exchanges and chemical reactions are slow (Woignier, Primera, and Hashmy 2006).

Fluid exchanges and chemical reactions are directly related to soil alteration processes, which in turn transform the initial structure through chemical processes (e.g., leaching, precipitation, cementation) and physical processes (e.g., consolidation, discharge) (Mitchell and Soga 2005). According to these authors, soil fabric refers to the geometric arrangement of particles, particle groups, and pore spaces, while structure encompasses fabric and the system of forces between particles that reflect all aspects of soil composition, history, current state, and environment.

It has been found that these secondary minerals, such as halloysite, allophane, and imogolite, form a cemented soil structure (Herrera 2006). Cementation is one of the most relevant chemical processes characteristic of residual soil formation, where the metallic oxides generated control soil particle bonding. According to some conceptual models, it has been established that iron oxides intervene in two important processes: a) they form an impermeable layer around clay particles, and b) they provide cementation bonds that keep the aggregate spheres rigid and the platelets together (Zhang et al. 2004). Figure 2 illustrates these two processes.

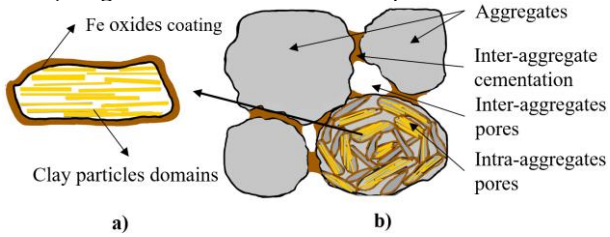

Figure 2. Conceptual representation of microstructural unit (Adapted from Zhang et al. 2004).

2. Background

2.1. Weathering degree

Weathering processes in soils start at the weakest bonds; therefore, it is possible to assess the degree of weathering of minerals by estimating the force through which oxygen binds to the most mobilizable elements, which corresponds to the alkali and alkaline-earth metals (Macías and Camps-Arbestain 2020).

Based on this principle, various authors have proposed expressions to evaluate the degree of weathering, whose results are termed the geochemical alteration index. Those indexes relate to chemical components that are less and more mobilizable to reflect the evolution and mineralogical changes of soil.

Table 1 presents the equations proposed by each author along with the optimal values for low and high alteration degrees. Below is the description of each index.

Ruxton, *R*: Relates silica loss to total element loss, considering aluminum (and other sesquioxides), which are immobile during weathering (Ruxton 1968). During the weathering process of volcanic ash, silica is released to form secondary minerals; therefore, the *R* index is a good indicator for evaluating alteration in these soils.

Parker Weathering Index, *WIP*: Based on the proportions of more mobile compounds corresponding to alkali and alkaline-earth metals: sodium, magnesium, potassium, and calcium. Takes into account the individual mobility of each compound based on the bonding forces with oxygen (Price and Velbel 2003; Parker 1970). It has been widely used in technical literature to research volcanic materials in Japan.

Weathering Product Index, *PWI*: Based on tracking the less mobile components: silica, aluminum, iron, and titanium. It is complemented by the Parker index to provide a system that reflects both the initial and advanced stages of weathering (Rajmi et al. 2021; Souri, Watanabe, and Sakagami 2006).

Vogt, *V*: Relates more mobile components, such as magnesium, calcium, and sodium, to less mobile components, such as aluminum and potassium. The relationship evaluates the weathering state of residual sediments (Vogt 1927).

Chemical Index of Alteration, *CIA*: Interprets a measure of the degree of degradation of feldspars that dominate the processes of chemical alteration in the most superficial zone of the parent material, with the corresponding formation of clays such as kaolinite (Fiantis et al. 2010; Fedo, Wayne, and Young 1995). According to the occurrence of minerals during weathering exposed in Figure 1, the index is representative of this type of soil because it considers the compounds in the formation of kaolinite.

Chemical Index of Weathering, *CIW*: It has the same compounds as CIA except that it eliminates potassium. Aluminum is considered the component with low mobility, and calcium and sodium as the most mobile because they leach easily. Potassium is not taken into account because it can leach or accumulate in the residue during erosion (Harnois and Moore 1988).

Plagioclase Alteration Index, *PIA*: It is an alternative measure to CIW, used in monitoring the erosion of plagioclase due to its ability to dissolve rapidly (Fedo, Wayne, and Young 1995).

Table 1. Weathering indices proposed by various authors (Adapted from Fiantis et al. 2010).

Index	Formula	Optimum Fresh Value	Optimum Weathered Value
R	$\frac{SiO_2}{Al_2O_3}$	10	0
WIP	$\left(\frac{2Na_2O}{0.35}+\frac{MgO}{0.9}+\frac{2K_2O}{0.25}+\frac{CaO}{0.7}\right)\times 100$	> 100	0
PWI	$\left(\frac{SiO_2}{TiO_2+Fe_2O_3+SiO_2+Al_2O_3}\right)\times 100$	> 50	0
V	$\frac{Al_2O_3+K_2O}{MgO+CaO+Na_2O}$	> 1	*Infinite*
CIA	$\left(\frac{Al_2O_3}{Al_2O_3+CaO+Na_2O+K_2O}\right)\times 100$	≤ 50	100
CIW	$\left(\frac{Al_2O_3}{Al_2O_3+CaO+Na_2O}\right)\times 100$	≤ 50	100
PIA	$\left(\frac{Al_2O_3-K_2O}{Al_2O_3+CaO+Na_2O-K_2O}\right)\times 100$	≤ 50	100

2.2. Dispersion

To assess soil erosion susceptibility, various tests have been proposed: flow pump test, channel erosion test, or pinhole erosion test. Among these tests, the most widely used is the pinhole erosion test, developed to evaluate soil dispersion susceptibility with a focus on dam construction (Nadal-Romero et al. 2011).

Some authors have indicated that particle size distribution and soil uniformity coefficient are important factors affecting erosion characteristics. For example, soils with grain sizes between 0.2 and 0.6 mm and uniform grain size distribution ($C_u < 2$) are more susceptible to erosion. This occurs because of the gaps between large particles that are not filled with small particles, thus leading to flow conditions conducive to dispersion processes (Dinh et al. 2021).

3. Materials and Experimental methods

3.1. Materials

Soil samples were obtained from a soil profile in the central-western region of Colombia, in the locality of Armenia, Quindío. The area is influenced by the tectonic evolution of the Central Cordillera, where volcanic activity from the Ruiz-Tolima complex has occurred. In the region, the geological unit called the "Quindío Fan" is identified, consisting of fluviovolcanic deposits: volcanic ash or fall pyroclasts with fine to medium grain size and ancient volcanic flows with residual soils (Servicio Geológico Colombiano 2004).

During the subsurface investigation, block undisturbed samples were extracted, from which three were selected to represent different degrees of weathering. The nomenclature used for these samples is as follows: (M1-5.30), (M2-5.80), and (M3-6.30), where the numerical value denotes the final depth of the sample. For this selection, mainly index properties and allophane content were considered. Table 2 presents the "index" properties and allophane content of the samples.

The allophane content was estimated using the equation established from the mass loss when exposing the sample to heating at 105°C and 200°C. This mass loss represents the value of (x) in Equation 1 (Kitagawa 1976). Allophane content can be related to the sequence of material evolution by the alteration sequence depicted in Figure 1.

$$Allophane\ content\ (\%) = (10.7 \times x) - 7 \qquad (1)$$

Table 2. Index properties of materials.

Index Properties	M1-5.30	M2-5.80	M3-6.30
Wc (%)	51.55	45.94	43.02
Gs	2.69	2.73	2.74
LL (%)	47.05	38.77	41.57
IP (%)	15.24	13.08	14.18
Sand (%)	46.05	60.18	71.95
Passing Sieve No.200 (%)	53.95	39.82	28.04
Allophane Content (%)	25.86	3.40	9.16

The characterization tests for index properties were conducted with some modifications to avoid material alterations. The consistency limits were determined without initial drying according to ASTM D4318-17 (ASTM 2017) and particle size analysis was performed using the wet method following ASTM D4943-18 (ASTM 2018). The structure and physical behavior of allophanic soils can be altered by drying processes, some of which are chemical and irreversible, and are reflected in the index properties resulting from particle size, plasticity, or particle density tests (Herrera 2006; Wesley 2003; Wesley 2009) These changes in properties can be caused by: alteration of clay minerals due to partial dehydration and aggregation of fine particles to form larger particles that remain bonded even upon rehydration (Geological Society Professional Handbooks 1990).

According to the literature, fine materials predominate in the presence of allophane. It agrees with the percentage of material passing through the No. 200 sieve identified in the samples. For example, in sample M1-5.30, a fines percentage of 53.95% was found, with the highest allophane content among the three samples at 25.86%.

In the plasticity chart, allophanic soils are typically found below the "A-line," and higher values of the liquid limit are observed as the allophane content increases (So 1998). As seen in Figure 3, sample M1-5.30 is further away from the "A-line" compared to specimen M2-5.80. This finding is consistent with the results obtained using the Kitagawa equation, where sample M1-5.30 exhibits higher allophane content compared to M2-5.80.

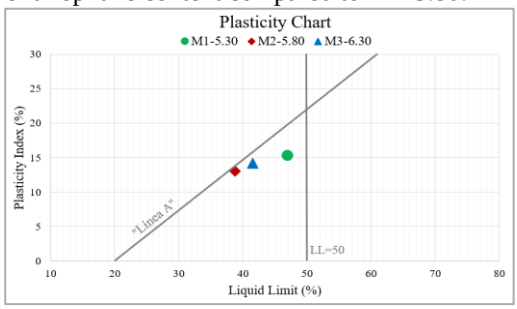

Figure 3. Location of the materials under study on the plasticity chart.

3.2. Experimental Methods

In order to study the soil chemistry and establish the degree of weathering, X-ray fluorescence spectroscopy (XRF) and scanning electron microscopy (SEM) tests were conducted on the selected samples. Additionally, to assess susceptibility to dispersion, the Pinhole test was performed.

3.2.1. X-Ray Fluorescence Spectrometry (XRF)

X-ray fluorescence spectrometry is a method that allows for the determination of the chemical composition of soils, and unlike other techniques, it does not require prior chemical preparation processes such as acid digestion (Marlborough District Council 2013). However, the results obtained through XRF are considered semi-quantitative because their precision does not match that of more rigorous analytical techniques such as atomic absorption spectroscopy.

For the test, the samples were dried at 105°C for 12 hours, ground to reduce particle size, passed through a 100µ mesh sieve, then mixed with spectrometric wax in a 10:1 ratio, homogenized by agitation, and finally pressed in a hydraulic press at 120 kN for one minute to generate a 37 mm diameter pellet. The MagixPro PW-2440 Philips equipment (WDXRF) and SemiQ 5 software were used.

3.2.2. Scanning Electron Microscopy (SEM)

Scanning electron microscopy produces images from signals resulting from the interaction of the electron beam with the sample. In combination with an energy-dispersive X-ray analyzer (EDX), it generates a mapping of the sample by analyzing elements near the surface and estimates the elemental proportion at different positions of the sample (Titus, James, and Roopan 2019).

For the test, the samples were previously dried at 105°C for 8 hours, then they were ground to reduce particle size and homogenized. The Q150R-ES Quorum equipment was used to coat the samples with a thin layer of gold to prevent static electricity buildup through conductivity. The EVO-HD15 Zeiss equipment, SmartSEM Touch, and SmartEDX software were used.

3.2.3. Pinhole Test

The "Pinhole" test method for assessing dispersion involves flowing distilled water, under different hydraulic heads through a 1mm diameter hole drilled in the soil sample. The coloration of the solution exiting the sample, the flow rate (flow rate), and the final size of the hole provide the criteria for classifying the dispersion of the soil samples. In this way, the test provides a direct, qualitative measure of dispersion and therefore the colloidal erodibility of soils (ASTM 2020).

The tests were carried out according to the procedures outlined in ASTM D4647 (ASTM 2020) for Method A, which classifies the specimen according to the following criteria summarized in Figure 4.

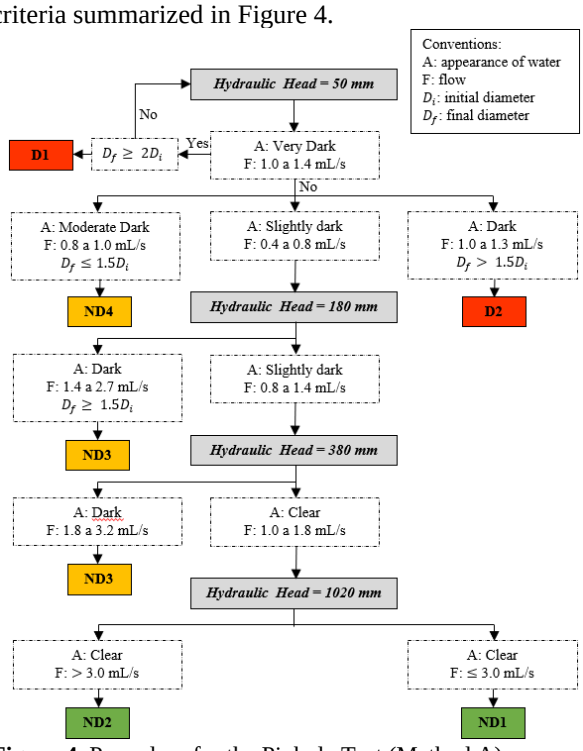

Figure 4. Procedure for the Pinhole Test (Method A).

Dispersion tests were conducted in both natural (N) and compacted (C) states. For the compacted samples, two tests were carried out: one with natural water content (CN) and another after air-drying of the sample (CD). Compacted samples were prepared into three successive layers with 8 blows per layer using a mass of 800 grams falling from a height of 30 cm.

4. Results and Discussion

Table 3 presents the results of the XRF and SEM tests. The values correspond to the weight percentages of chemical compounds.

Table 3. Composition Results from XRF and SEM Tests.

Sample	Oxide	XRF (%)	SEM (%)
M1-5.30		46.04	43.28
M2-5.80	SiO_2	46.61	31.30
M3-6.30		44.95	22.88
M1-5.30		25.02	27.02
M2-5.80	Al_2O_3	25.93	22.88
M3-6.30		26.07	17.51
M1-5.30		1.08	1.53
M2-5.80	Na_2O	1.32	1.67
M3-6.30		0.96	0.81
M1-5.30		1.39	2.35
M2-5.80	MgO	0.80	0.58
M3-6.30		1.50	1.23
M1-5.30		0.82	0.93
M2-5.80	K_2O	0.59	0.43
M3-6.30		0.92	0.46
M1-5.30		3.19	2.09
M2-5.80	CaO	3.34	1.44
M3-6.30		2.93	1.00
M1-5.30		0.97	1.60
M2-5.80	TiO_2	0.83	1.11
M3-6.30		0.96	0.67
M1-5.30		5.95	11.17
M2-5.80	Fe_2O_3	5.00	8.23
M3-6.30		6.12	4.64

The difference in values obtained between XRF and SEM is evident. This is because SEM analyzes the composition using an energy-dispersive X-ray analyzer (EDX) on specific sections of the sample rather than the totality, as done by XRF.

For sample M1-5.30, the results for Fe_2O_3 varied between the two methods, ranging from 5.95% to 11.17%. The readings obtained with SEM identified ferruginous concretions elevating the content of this oxide. Figure 5 illustrates the image obtained for the sample, showing particle aggregation with a smooth, uniform surface characteristic of iron oxide coating.

Regarding the results of TiO_2 for sample M1-5.30, the values range from 0.97% to 1.60%. In Figure 5, it is evident that TiO_2 concentrates in the same sectors of the sample as Fe_2O_3. This can be explained because titanium and iron oxides accumulate under the same conditions, forming surface coatings on aggregates (Sherman 1952). Additionally, once titanium is in solution, it becomes masked within iron-containing minerals, as iron and titanium have similar ionic sizes (Mclaughlin 1954).

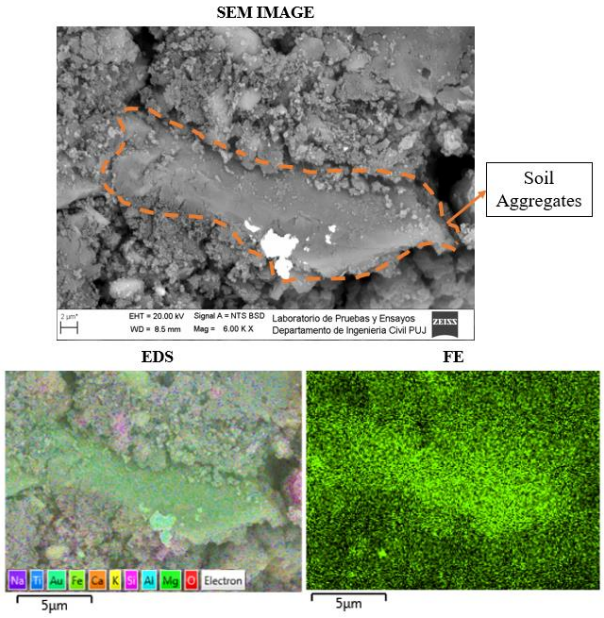

Figure 5. SEM Results for Sample M1-5.30

Regarding the results obtained for the alkali and alkaline-earth compounds, it was found that they vary considerably. For example, for specimen M3-6.30, the result for CaO varies from 2.93% to 1.00%. It is important to consider that calcium, potassium, magnesium, and sodium oxides contribute to the exchangeable cations in the soil, playing a crucial role in mineral alteration processes due to their ability to be replaced by soil solution. For this reason, they are considered in the *WIP*, *V*, *CIA*, *CIW*, and *PIA* indices as the most mobilizable components.

The compounds that showed the greatest difference in results between SEM and XRF tests were Fe_2O_3, TiO_2 and CaO. For the evaluation of geochemical indices (see Table 2), *PWI* is the only one that considers Fe_2O_3 and TiO_2, while CaO is considered for the *WIP*, *V*, *CIA*, *CIW* and *PIA* indices.

Taking the above into account, it is evident that the estimation of the geochemical index is significantly affected by using results from one technique or the other. For example, for sample M3-6.30, the *WIP* index obtained with XRF values is 23.84, while with SEM values it is 13.58. This would lead to interpretations of higher and lower weathering, respectively. However, this variation in results is due to the differential estimation of alkaline earth compounds obtained by each technique.

The weathering indices were determined using the XRF results, and these are presented in Table 4.

Table 4. Weathering indices defined with XRF.

Weathering Index	M1-5.30	M2-5.80	M3-6.30
R	1.84	1.80	1.72
WIP	23.90	21.81	23.84
PWI	59.47	59.04	57.55
V	4.57	4.86	5.01
CIA	83.10	83.16	84.42
CIW	85.42	84.77	87.02
PIA	85.00	84.47	86.60

For the *R* index, sesquioxides are considered constant during mineral alteration, which is not always the case. However, for the three analyzed samples, a maximum variation of 4% in the content of Al_2O_3 was found, so the validity of this assumption is assumed for this case. Figure 6 presents the results with the *R* index, where the samples are defined from highest to lowest degree of weathering as follows: M3-6.30, M2-5.80, and M1-5.30. For the *V* index, which includes alkaline-earth compounds as mobilizable, the trend presented in *R* is maintained, as evidenced in Figure 6.

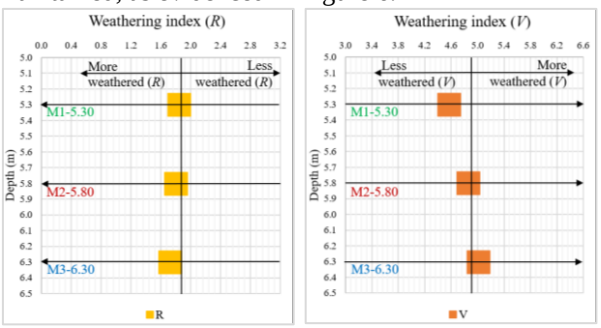

Figure 6. Results of *R* and *V* indices for samples M1-5.30, M2-5.80, and M3-6.30.

The results of *PWI* align with the trend obtained in the *R* and *V* indices. However, in the *WIP* results, this trend shifts to M2-5.80, M3-6.30, and M1-5.30. This change could be explained by the influence of the values established to relate the mobility of each compound based on its bonding forces with oxygen.

Figure 7 presents the relationship between WIP and PWI. Some authors defined a linear correlation coefficient R of 0.505 for less weathered soils and 0.871 for more weathered soils in allophanic soils from Japan (Souri, Watanabe, and Sakagami 2006). According to this, the samples under study, compared to those presented by these authors, exhibit a lower degree of alteration with a linear correlation coefficient R of 0.420.

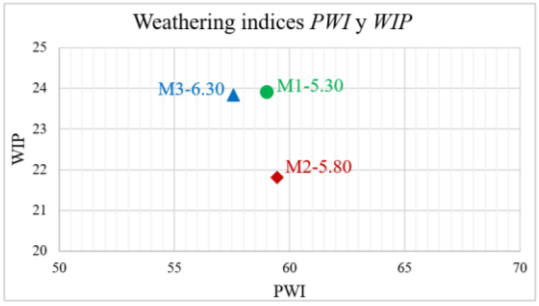

Figure 7. Relationship between *PWI* and *WIP* indices for samples M1-5.30, M2-5.80, and M3-6.30.

The results for *CIA*, *CIW*, and *PIA* are presented in Figure 8. It is important to mention that these indices use the same compounds with some modifications by considering K_2O. These indices follow the weathering trend obtained for R, V, and PWI.

Taking the above into account, six out of the seven indices show the same trend of weathering in the samples; from highest to lowest degree: M3-6.30, M2-5.80, and M1-5.30. The *WIP* index is the only one that represents a different trend of weathering degree.

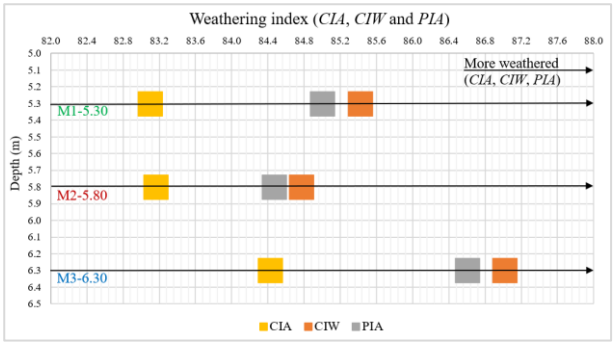

Figure 8. Results of *CIA*, *CIW*, and *PIA* indices for samples M1-5.30, M2-5.80, and M3-6.30.

Figure 9 presents the results obtained for the Pinhole test in terms of dry density for each sample and permeability for each of the hydraulic heads of 0.18, 0.38, and 1.020 m (the three points for each line, respectively).

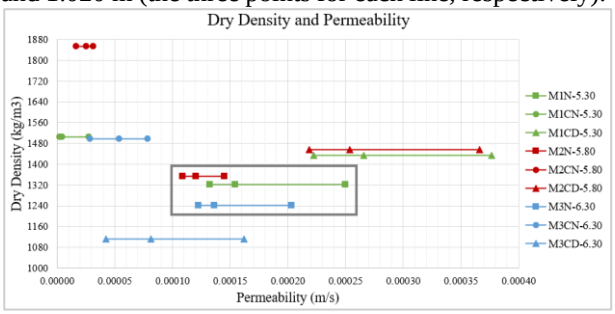

Figure 9. Permeability results in the Pinhole test for samples M1-5.30, M2-5.80, and M3-6.30.

The natural samples shown in the gray rectangle of Figure 9 exhibit a particular behavior. Although they have the lowest dry densities, indicating more open and porous structures, they do not exhibit the highest permeabilities. According to (Woignier, Primera, and Hashmy 2006), this can be explained by the analogy between gels and allophane aggregates, which strongly affect properties such as permeability, resulting in very low values caused by particle aggregation. This particle aggregation may be related to cementation processes that hinder the connection between pores in natural samples, thus resulting in lower permeability compared to compacted samples.

The most weathered sample (M3N-6.30) shows lower dry density and higher sand content. Normally, this condition promotes internal erosion processes. However, as observed in Figure 10, this sample exhibits lower porosity, indicating that the filling and cementing minerals are stable and maintain the soil structure, preventing susceptibility to erosion as reflected in the low permeability values. On the other hand, the least weathered sample (M1N-5.30) has higher dry density, greater porosity, and is more susceptible to erosion due to the lack of cementation.

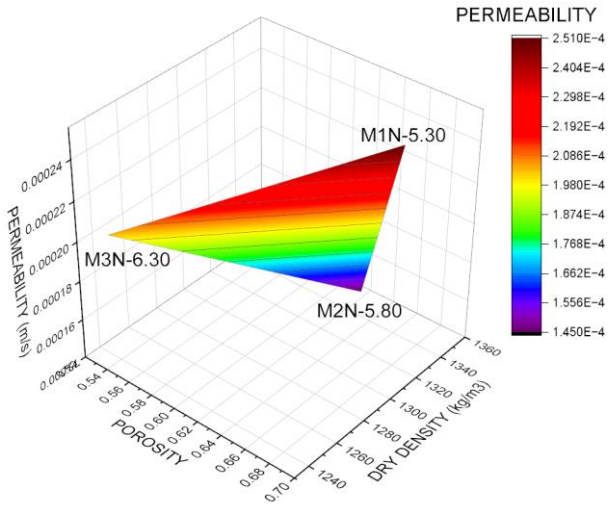

Figure 10. Relation of porosity, dry density, and permeability for natural samples M1-5.30, M2-5.80 y M3-6.30.

In compacted samples, the alteration of the material due to drying generates differences in porosity and hydraulic conductivity when comparing samples dried in air versus samples dried in an oven. It is inferred that the drying process at higher temperatures changes the properties of the material, eliminating the "gel texture" and therefore the cementing bonds. In Figure 11, a drastic change in permeability values at constant porosity and dry density is evident for some samples, demonstrating a clear variation in macro- and microporosity. Additionally, a critical dry density of 1480 kg/m3 is identified for these samples, beyond which the permeability values vary considerably.

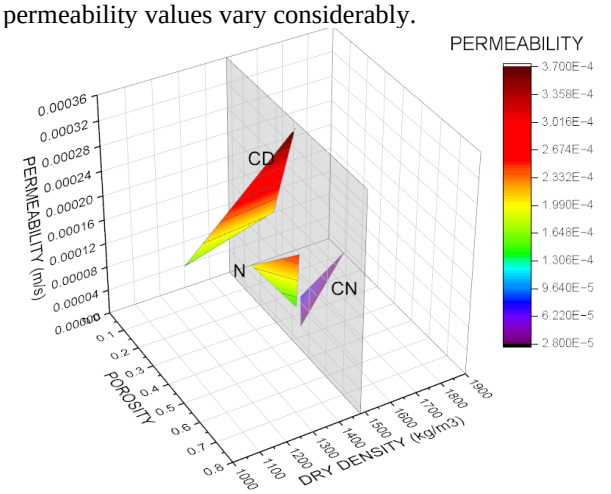

Figure 11. Relationship between porosity, dry density, and permeability for natural and compacted samples (air-dried and oven-dried).

The flow rates in the conducted tests do not exceed 0.003l/s. Therefore, according to ASTM4647, all three types of materials under natural and compacted conditions are classified as non-dispersive soils ND1. Regarding the coloration of the solution exiting the sample, it remains "clear" for all tests, even when high permeability values are observed.

5. Conclusions

The trends indicating the degree of weathering through different geochemical indices converge in the results, showing the following order of increasing

alteration for the three samples: M3-6.30, M2-5.80, and M1-5.30.

The sequence of mineral alteration shown in Figure 1 does not imply that the most weathered material has a higher fine content. It is interpreted that cementation and alteration occur in some areas of the material mass. Therefore, sample M3, despite having a lower fine content, promotes a higher degree of alteration in the analysis results.

For natural samples in allophanic soils, aggregations similar to gels are formed, showing a particular behavior. With low dry densities, permeability values are low, explained by cementation that reduces infiltration capacity. Therefore, it is possible to associate the degree of alteration with susceptibility to dispersion. A lower degree of alteration corresponds to greater susceptibility to internal erosion, where cementing bonds with gel texture have not yet formed, allowing pore connection.

For oven-dried compacted samples, higher permeability is observed compared to those air-dried. It is inferred that higher drying temperatures alter the gel properties inherent to the natural material and the cementing bonds identified in aggregates with high contents of Fe_2O_3 and TiO_2.

In allophanic soils, higher ranges of compaction energy drastically reduce the permeability of the materials. This process is associated with the remolding and alteration of clay minerals, rather than the particle rearrangement (density) process. Despite having a lower content of fines compared to other samples, the M3-6.30 sample exhibits a higher degree of alteration. Similarly, it showed less susceptibility to remolding, as evidenced by the lack of changes in the pinhole tests for both compacted and natural samples. This could be attributed to the aggregates forming cementation bonds that reduce infiltration capacity.

Acknowledgments

The authors are grateful to Dr. Gina Marcela Hincapié Triviño, professor at the Department of Chemistry at UNAL, for her guidance and support. Additionally, they acknowledge the support provided by the professionals at the X-ray Fluorescence Laboratory (UNAL) and the Scanning Electron Microscopy Laboratory (PUJ).

References

ASTM. 2017. “D4318: Standard Test Methods for Liquid Limit, Plastic Limit, and Plasticity Index of Soils.” In , 1–7. https://doi.org/10.1520/D4318-17E01.

———. 2018. “D4943: Standard Test Method for Shrinkage Factors of Cohesive Soils by the Water Submersion Method.” In , 1–3. https://doi.org/10.1520/D4943-18.

———. 2020. “D4647: Standard Test Methods for Identification and Classification of Dispersive Clay Soils by the Pinhole Test.” In . https://doi.org/10.1520/D4647_D4647M-13R20.

Dinh, B., A. Nguyen, S. Jang, and Y. Kim. 2021. “Evaluation of Erosion Characteristics of Soils Using the Pinhole Test.” International Journal of Geo-Engineering 12 (1): 16. https://doi.org/10.1186/s40703-021-00145-4.

Fedo, M., H. Wayne, and M. Young. 1995. “Unraveling the Effects of Potassium Metasomatism in Sedimentary Rocks and Paleosols, with Implications for Paleoweathering Conditions and Provenance.” Geology 23 (10): 921. https://doi.org/10.1130/0091-7613(1995)023<0921:UTEOPM>2.3.CO;2.

Fiantis, D., M. Nelson, J. Shamshuddin, T. Goh, and E. Van. 2010. “Determination of the Geochemical Weathering Indices and Trace Elements Content of New Volcanic Ash Deposits from Mt. Talang (West Sumatra) Indonesia.” Eurasian Soil Science 43 (13): 1477–85. https://doi.org/10.1134/S1064229310130077.

Flórez, M., and L. Parra. 2009. “Characteristics of Alteration in Minerals of Volcanic Ashes of the North of the ‘Cordillera Central’ of Colombia.” Boletin de Ciencias de La Tierra 27: 49–70.

Gasser, U., S. Juchler, and H. Sticher. 1994. “Chemistry and Speciation of Soil Water from Serpentinitic Soils.” Soil Science 158 (5): 314–22. https://doi.org/10.1097/00010694-199411000-00002.

Geological Society Professional Handbooks. 1990. “Tropical Residual Soils Geological Society Engineering Group Working Party Report.” Quarterly Journal of Engineering Geology 23 (1): 4–101. https://doi.org/10.1144/GSL.QJEG.1990.023.001.01.

Harnois, L., and J. Moore. 1988. “Geochemistry and Origin of the Ore Chimney Formation, a Transported Paleoregolith in the Grenville Province of Southeastern Ontario, Canada.” Chemical Geology 69 (3–4): 267–89. https://doi.org/10.1016/0009-2541(88)90039-3.

Herrera, M. 2006. “Suelos Derivados de Cenizas Volcánicas En Colombia: Estudio Fundamental e Implicaciones En Ingeniería.” https://repositorio.uniandes.edu.co/bitstream/handle/1992/7812/u277084.pdf?sequence=1&isAllowed=y.

Kitagawa, Y. 1976. “Determination of Allophane and Amorphous Inorganic Matter in Clay Fraction of Soils.” Soil Science and Plant Nutrition 22 (2): 137–47. https://doi.org/10.1080/00380768.1976.10432975.

Macías, F., and M. Camps-Arbestain. 2020. “A Biogeochemical View of the World Reference Base Soil Classification System.” Advances in Agronomy 160 (1): 295–342. http://dx.doi.org/10.1016/bs.agron.2019.11.002.

Marlborough District Council. 2013. “Analysis of Soil Samples Using a Portable X-Ray Fluorescence Spectrometry (XRF) Marlborough District Council Solutions for Your Environment,” 14. https://docplayer.net/19500160-Analysis-of-soil samples-using-a-portable-x-ray-fluorescence-spectrometry-xrf.html.

Mclaughlin, R. 1954. “Iron and Titanium Oxides in Soil Clays and Silts.” Geochimica et Cosmochimica Acta 5 (2): 85–96. https://doi.org/10.1016/0016-7037(54)90043-5.

Mitchell, J, and K. Soga. 2005. Fundamentals of Soil Behavior. Third Edition. Wiley.

Nadal-Romero, E., E. Verachtert, R. Maes, and J. Poesen. 2011. “Una Nueva Herramienta Para Evaluar La Susceptibilidad de Los Suelos a Los Procesos de Sufosión o Piping : El Pinhole Test.” Cuadernos de Investigación Geográfica 37 (1): 99–114. https://doi.org/10.18172/cig.1248.

Parfitt, R. L. 2009. “Allophane and Imogolite: Role in Soil Biogeochemical Processes.” Clay Minerals 44 (1): 135–55. https://doi.org/10.1180/claymin.2009.044.1.135.

Parker, A. 1970. “An Index of Weathering for Silicate Rocks.” Geological Magazine 107 (6): 501–4. https://doi.org/10.1017/S0016756800058581.

Price, J., and M. Velbel. 2003. “Chemical Weathering Indices Applied to Weathering Profiles Developed on Heterogeneous Felsic Metamorphic Parent Rocks.” Chemical Geology 202 (3–4): 397–416. https://doi.org/10.1016/j.chemgeo.2002.11.001.

Rajmi, S., G. Gusnidar, R. Lubis, F. Ginting, F. Hidayat, H. Zulhakim, A. Armer, N. Yulanda, I. Syukri, and D. Fiantis. 2021. “Improving Volcanic Soil Chemistry After the Eruption of Mt. Sinabung, North Sumatera in 2020.” IOP Conference Series: Earth and Environmental Science 757 (1): 012042. https://doi.org/10.1088/1755-1315/757/1/012042.

Ruxton, B. 1968. “Measures of the Degree of Chemical Weathering of Rocks.” The Journal of Geology 76 (5): 518–27. https://doi.org/10.1086/627357.

Servicio Geológico Colombiano. 2004. “Cartografía Geológica Aplicada a La Zonificación Geomecánica Del Departamento Del Quindío. Volumen II.” SGC.

Sherman, G. 1952. “The Titanium Content of Hawaiian Soils and Its Significance.” Soil Science Society of America Journal 16 (1): 15–18. https://doi.org/10.2136/sssaj1952.03615995001600010006x.

Shoji, S., M. Nanzyo, and R. Dahlgren. 1993. “Chapter 8 Productivity and Utilization of Volcanic Ash Soils.” Developments in Soil Science 21 (C): 209–51. https://doi.org/10.1016/S0166-2481(08)70269-1.

Smeck, N., E. Runge, and E. Mackintosh. 1983. Pedogenesis and Soil Taxonomy - II. The Soil Orders. Pedogenesis and Soil Taxonomy. Vol. 11. Developments in Soil Science. Elsevier. https://doi.org/10.1016/S0166-2481(08)X7022-9.

So, E. 1998. “Statistical Correlation between Allophane Content and Index Properties for Volcanic Cohesive Soil.” Soils and Foundations 38 (4): 85–93. https://doi.org/10.3208/sandf.38.4_85.

Souri, B., M. Watanabe, and K. Sakagami. 2006. “Contribution of Parker and Product Indexes to Evaluate Weathering Condition of Yellow Brown Forest Soils in Japan.” Geoderma 130 (3–4): 346–55. https://doi.org/10.1016/j.geoderma.2005.02.007.

Titus, D., E. James, and S. Roopan. 2019. “Nanoparticle Characterization Techniques.” In Green Synthesis, Characterization and Applications of Nanoparticles, 303–19. Elsevier. https://doi.org/10.1016/B978-0-08-102579-6.00012-5.

Vogt, T. 1927. “The Geology and Petrography of the Sulitjelma Field.” Norges Geologiske Undersökelse 121. https://www.scirp.org/reference/referencespapers?referenceid=2143364.

Wesley, L. 2003. “Geotechnical Characterisation and Behaviour of Allophane Clays.” Proc. International Workshop on Characterisation and Engineering Properties of Natural Soils 2: 1379–99. http://scholar.google.com/scholar?hl=en&btnG=Search&q=intitle:Geotechnical+characterisation+and+behaviour+of+allophane+clays#0.

———. 2009. “Behaviour and Geotechnical Properties of Residual Soils and Allophane Clays.” Obras y Proyectos 6: 5–10. https://www.academia.edu/23592251/Behaviour_and_geotechnical_properties_of_residual_soils_and_allophane_clays.

Woignier, T., J. Primera, and A. Hashmy. 2006. “Application of the DLCA Model to ‘Natural’ Gels: The Allophanic Soils.” Journal of Sol-Gel Science and Technology 40 (2–3): 201–7. https://doi.org/10.1007/s10971-006-7593-6.

Zhang, G., J. Germaine, A. Whittle, and C. Ladd. 2004. “Index Properties of a Highly Weathered Old Alluvium.” Géotechnique 54 (7): 441–51. https://doi.org/10.1680/geot.2004.54.7.441.